JOURNAL OF MATERIALS SCIENCE 14 (1979) 2818–2824

The influence of grain size, stress and temperature on the steady state creep of a 25 Cr–20 Ni austenitic stainless steel without precipitates

Y. TAKAHASHI, T. YAMANE
Department of Materials Science and Engineering, Osaka University, Suita 565, Japan

This work was performed in order to study the steady state creep behaviour of a modified 25 Cr–20 Ni stainless steel which has no precipitates. The test temperature range was 1171 to 1211 K, the stress range 4.9 to 19.6 MPa, and the grain size was 40 to 600 μm. The steady state creep rate, $\dot{\epsilon}_s$, decreases with increase in grain size, especially at the lowest stress; $\dot{\epsilon}_s$ is proportional to $1/d^2$ at 4.9 MPa, where d is a mean grain diameter. The variation of $\dot{\epsilon}_s$ with grain size is smaller in the middle and coarse-grained specimens than in the fine-grained specimens, the stress exponent, n, gradually decreases from ~ 4 to ~ 1.5 with reducing stress, but in the middle- and coarse-grained specimens, a discontinuous point appears on a log $\dot{\epsilon}_s$ versus log σ plot. The activation energy for the steady state creep of the coarse-grained specimens tends to be larger than that of the fine-grained specimens, and the tendency is remarkable in the higher stress level. It is indicated that the creep mechanisms in the fine-grained specimens are essentially different from those in the coarse-grained specimens, and that the creep at the lowest stresses and smallest grain size is similar to that predicted by a vacancy creep model involving grain-boundary diffusion.

1. Introduction

It is known that the creep properties of 25 Cr–20 Ni stainless steels are affected by carbide precipitates and sigma phase rather than grain size [1–5], so there have been few studies on the grain-size dependence of the steady state creep rate, $\dot{\epsilon}_s$. However, in view of the role of grain boundaries in several theories of high temperature creep [6–9], it is important to study the grain-size dependence of $\dot{\epsilon}_s$ even for the high temperature creep of the stainless steels.

In this paper, the dependence of $\dot{\epsilon}_s$ on grain size for a modified 25 Cr–20 Ni austenitic stainless steel was studied under the condition without carbide precipitates and sigma phase. The test temperatures were around 0.7 T_m* and the stress range was from 4.9 to 19.6 MPa. The other creep tests for a type 310 stainless steel were performed at 1171 K to be compared with the above work.

2. Experimental procedure

The chemical compositions of a vacuum-melted austenitic stainless steel and that of a type 310 stainless steel are shown in Table I. In the vacuum-melted stainless steel, the content of nickel was higher and that of chromium was lower than those of the type 310 stainless steel for the purpose of preventing carbide precipitation and sigma-phase formation.

The specimens with a gauge length of 50 mm and a diameter of 2.0 mm were made from cold drawn wires, and annealed as shown in Table II.

*T_m is an absolute solidus temperature of the alloy in the equilibrium diagram of Fe–Cr–Ni system (Shafmeister and Ergang).

0022–2461/79/122818–07$02.70/0

TABLE I Chemical compositions (wt%) of stainless steels

	Cr	Ni	C	Mn	Si	Cu	P
Vacuum-melted stainless steel	22.00	21.81	0.01	Nil	0.06	0.002	0.007
Type 310 stainless steel	25.50	19.2	0.051	1.43	0.49	–	0.008

The secondary treatments at each test temperature for 15 h followed the primary treatments. All heat treatments were done under a vacuum atmosphere. The mean grain diameters, d, were measured by the grain intercept method [10, 11]. In the case of a vacuum-melted austenitic stainless steel, it was impossible to obtain a proper grain size smaller than 40 μm for grain growth during the secondary treatment or creep tests. All specimens were crept in air by the uniaxial tensile stress after heating for 1 h at the test temperature. The stress was applied by a weight. The elongation was measured by a dial gauge to an accuracy of $\frac{1}{100}$ mm.

The test temperature and stress range were respectively 1171 to 1211 K and 4.9 to 19.6 MPa. The temperature was established to within ±0.5 K during the period of each test and the gradient along the specimen was controlled to within 1 K. Optical microstructures of the steady state creep stage were observed in the specimens that were cooled under load after creep. In the creep of the vacuum-melted austenitic stainless steel, the absence of precipitates was verified by electron transmission metallography.

3. Results

3.1. Vacuum-melted stainless steel

3.1.1. Influence of grain size on creep curves

Fig. 1 shows the creep curves of specimens with the mean diameters of 40, 80 and 600 μm. The creep curves for the coarse-grained specimens have a primary creep of the inverse type in the stress range 14.7 to 19.6 MPa, but under the lower stress level ($\leqq$ 9.8 MPa) they have an incubation period. Those for the fine-grained specimens are the normal creep curve at the stresses below 14.7 MPa, and the linear at 19.6 MPa.

Regardless of the aspect in the primary creep stage, the steady state creep stage follows in all creep curves.

TABLE II Heat treatments and mean grain diameters

Mean grain diameter (μm)	Primary heat treatment	Secondary heat treatment
40	1 h 1258 K	15 h at test temperatures and air-cooled
50	1 h 1323 K	
80	1 h 1373 K	
160	2.5 h 1473 K	
600	0.5 h 1573 K	

3.1.2. Grain-size dependence of the steady state creep rate

The following modified equation can be applied for the steady state creep [12, 13].

$$\dot{\epsilon}_s = A d^p \sigma^n \exp(-Q_c/RT) \qquad (1)$$

where A is a constant, d the mean grain diameter, p the grain diameter exponent, σ the creep stress, n the stress exponent, Q_c the activation energy for creep, R the gas constant, and T is the absolute temperature.

The variation of p is represented by $\log \dot{\epsilon}_s$ versus $\log d$ plots under the constant stress and temperature, as shown in Figs. 2, 3 and 4. The steady state creep rates monotonically decrease with increase in grain size. In the results for $\sigma = 4.9$ MPa, p is equal to -2 and the relationship of $\dot{\epsilon}_s \propto d^{-2}$ is established at all test temperatures. The effect of grain size is poor in the coarse-grained specimens at 9.8 MPa $\leqq \sigma \leqq$ 19.6 MPa; p gradually increases from -2 to $-\frac{1}{2}$ with grain size, except for the results at 1211 K. Similar decrease in the absolute value of p is found in other papers [10, 14], and may be due to the subgrains developing during the primary creep. In this work, however, few subgrains were observed by the transmission electron microscope.

3.1.3. Stress dependence of the steady state creep rate

The stress dependences of $\dot{\epsilon}_S$ are commonly represented on a $\log \dot{\epsilon}_s$ versus $\log \sigma$ plot [15–17].

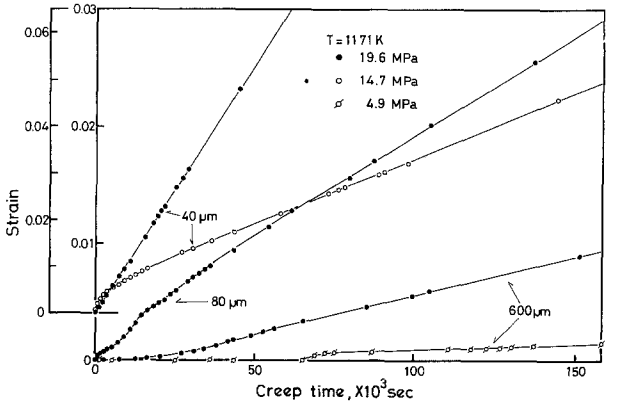

Figure 1 Creep curves for vacuum-melted stainless steel.

The present results are also arranged in this form. The slopes (n) of the curves for 40, 50 and 80 μm in Fig. 5 change from ~1.5 to ~4 with stress, but those for 160 and 600 μm have, discontinuously, the value of about 5 in the lower stress range. These may be explained by the theories of Crossman and Ashby [8] or Gifkins [9].

3.1.4. Grain-size dependence of the activation energy for creep

The temperature dependence of $\dot{\epsilon}_S$ at each grain size is shown in Fig. 6. The data for 80 μm under 9.8 MPa $\leqq \sigma \leqq$ 19.6 MPa cannot be fitted to a straight line. The temperature dependence of $\dot{\epsilon}_S$ in the coarse-grained specimens increases with increasing stress.

The relationship of the activation energy, Q_c, for creep and d is illustrated in Fig. 7. Q_c is given by Equation 2.

$$Q_c = -R \left(\frac{\partial \ln \dot{\epsilon}_S}{\partial \ln 1/T} \right)_{\sigma,d} \tag{2}$$

It has been said that Q_c is essentially insensitive to a change in grain size for the creep in austenitic stainless steels [6, 18]. In this work, however, the results give evidence of the influence of the grain

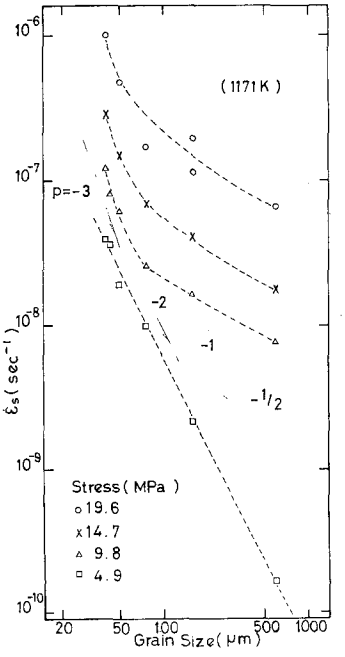

Figure 2 Grain-size dependence of $\dot{\epsilon}_S$ at 1171 K for vacuum-melted stainless steel.

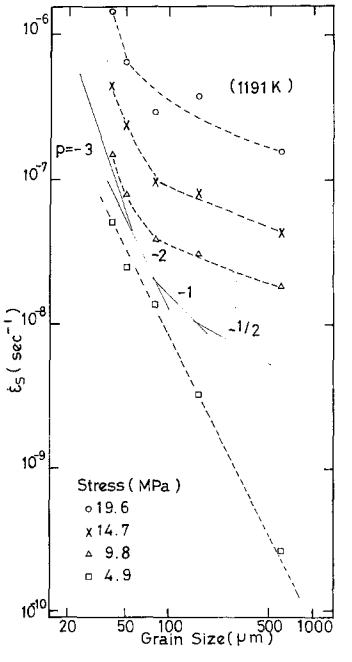

Figure 3 Grain-size dependence of $\dot{\epsilon}_S$ at 1191 K for vacuum-melted stainless steel.

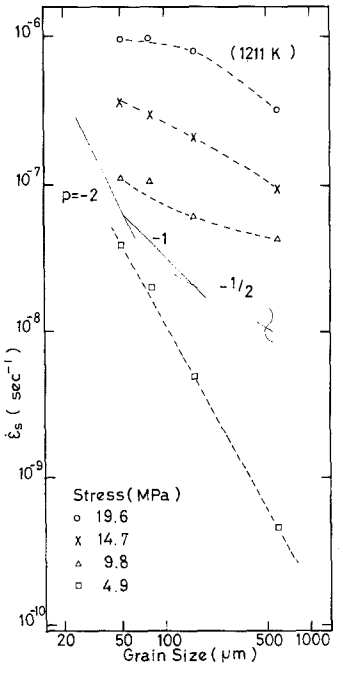

Figure 4 Grain-size dependence of $\dot{\varepsilon}_s$ at 1211 K for vacuum-melted stainless steel.

size on the activation energy. It suggests that the creep process in the fine-grained specimens is different from that in the coarse-grained specimens. In the fine-grained specimens, Q_c is in agreement with the activation energy of the grain-boundary self-diffusion of Fe in the Fe–Cr–Ni system [19]. In the coarse-grained specimens, Q_c obtained for $\sigma = 4.9$ MPa is nearly equal to that of the volume self-diffusion of Fe [19], and Q_c under the stress condition of $9.8\,\text{MPa} \leqq \sigma \leqq 19.6\,\text{MPa}$ has large values of 400 to 500 kJ mol^{-1}.

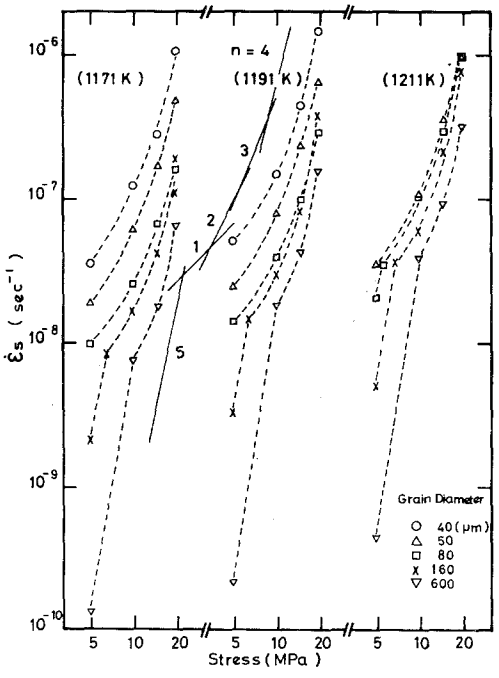

Figure 5 Stress dependence of $\dot{\varepsilon}_s$ for vacuum-melted stainless steel.

3.1.5. Microstructure

No precipitates are observed after the creep for the vacuum-melted austenitic stainless steel. The remaining twin boundaries are observed in the fine-grained specimens, in contrast to the coarse-grained specimens, as seen in Fig. 8. It is suggested that the deformation within grains is reduced in the fine-grained specimens. No grain growth occurs at either 1171 or 1191 K. The creep tests for 40 μm could not be performed at 1211 K for grain growth. This indicates that the migration of grain boundaries begins at 1211 K, so that the results for $9.8\,\text{MPa} \leqq \sigma \leqq 19.6\,\text{MPa}$ at 1211 K are different from those at 1171 or 1191 K.

3.2. Type 310 stainless steel

The creep tests for a type 310 stainless steel were carried out in air, to enable comparison with the experiments on the vacuum-melted austenitic stainless steel.

Fine-grained specimens below 40 μm could be obtained. On the other hand, the tests for the coarse-grained specimens could not be performed, since the strain rate was immeasurably small. The precipitates were observed in the grain boundaries and within grains after all creep tests. The results for the type 310 stainless steel are shown in Figs. 9 and 10. In the fine-grained specimens, the precipitates do not appear to influence creep behaviour, as much as in the steady state creep region.

4. Discussion

It is usually recognized that under conditions of low stress and small grain size, and at temperatures higher than $0.5\,T_m$, creep takes place by the stress-directed diffusion of vacancies either through the lattice or along the grain boundaries [7, 20–24]. In this case, experimental results should be in agreement with the diffusional creep equation [7, 20]:

$$\dot{\varepsilon}_s = 14 \cdot \frac{\sigma\Omega}{kT} \cdot \frac{1}{d^2} D_v \left(1 + \frac{\pi\delta}{d} \cdot \frac{D_b}{D_v}\right), \quad (3)$$

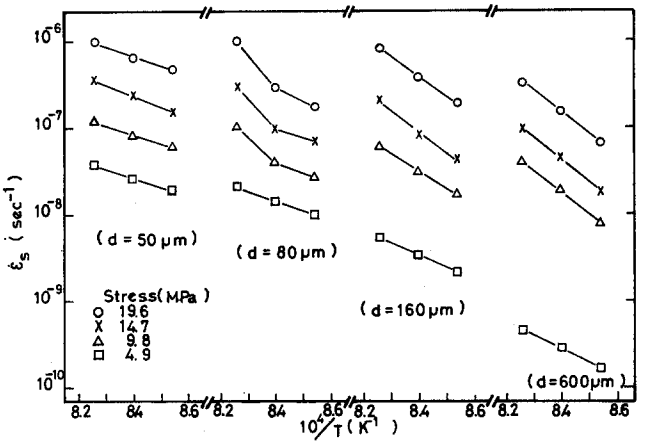

Figure 6 Temperature dependence of $\dot{\varepsilon}_s$ for vacuum-melted stainless steel.

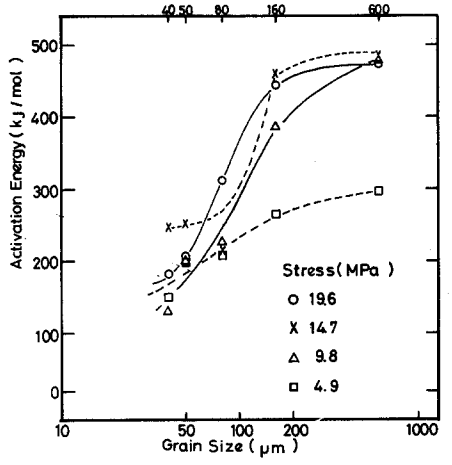

Figure 7 Grain-size dependence of the activation energy for the creep in vacuum-melted stainless steel. The experimental points for 80 μm at 9.8 MPa $\leqq \sigma \leqq$ 19.6 MPa are made from the data in the lower temperature region of 1171 to 1191 K.

where Ω is the atomic volume, k Boltzman's constant, δ the effective grain-boundary width, $D_v = D_{vo} \exp(-Q_v/RT)$, the volume self-diffusion coefficient with a pre-exponential constant, D_{vo} and an activation energy, Q_v; and $D_b = D_{bo} \exp(-Q_b/RT)$, the grain-boundary self-diffusion coefficient with a pre-exponential constant, D_{bo} and an activation energy, Q_b.

In this work, the present results at the lowest stresses and smallest grain sizes give strain rates nearly equal to that predicted by Equation 3 within a factor of 2, and indicate that the diffusional creep along the grain boundaries dominates*. This is supported by the fact that $p = -2$ to -3, $n \simeq 1.5$, $Q_c \simeq 180\,\mathrm{kJ\,mol^{-1}}$ in the fine-grained specimens.

On the other hand, in the middle- and coarse-grained specimens, the total strain results from

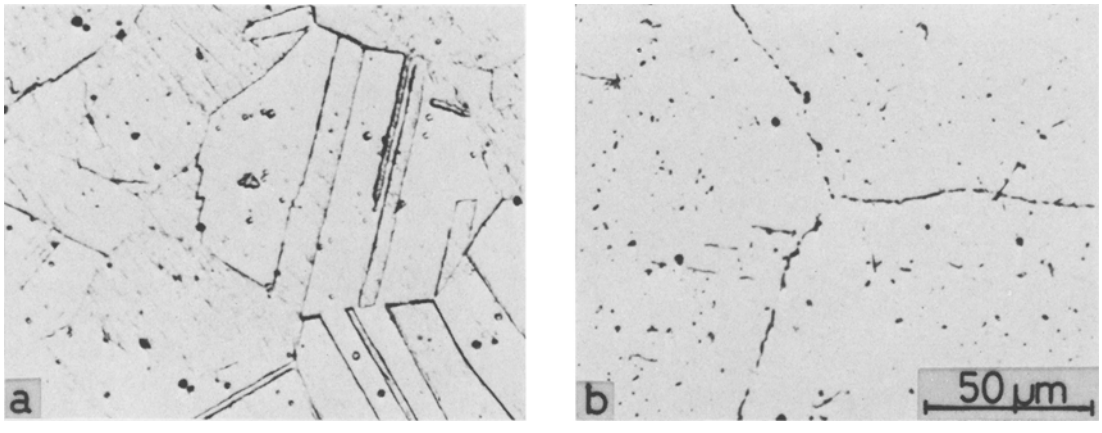

Figure 8 Optical microstructures: (a) 1191 K, 14.7 MPa, 50 μm; (b) 1191 K, 14.7 MPa, 600 μm.

*With $\Omega = 1.21 \times 10^{-29}$ m^3 [11], $\delta \times D_{bo} = 8.3 \times 10^{-13}$ m^3 sec^{-1}, $Q_b = 180$ kJ mol^{-1}, $D_{vo} = 1.74 \times 10^{-4}$ m^2 sec^{-1}, $Q_v = 284$ kJ mol^{-1} [19], and $d = 40\,\mu$m, $\dot{\varepsilon}_s = 2.0 \times 10^{-8}$ sec^{-1} at $\sigma = 4.9$ MPa, $T = 1171$ K is obtained from Equation 3 where the first term gives 1.2×10^{-9} sec^{-1}. $\dot{\varepsilon}_s$, which was measured at $\sigma = 4.9$ MPa, $T = 1171$ K, $d = 40\,\mu\mathrm{m} = 3.9 \times 10^{-8}$ sec^{-1}.

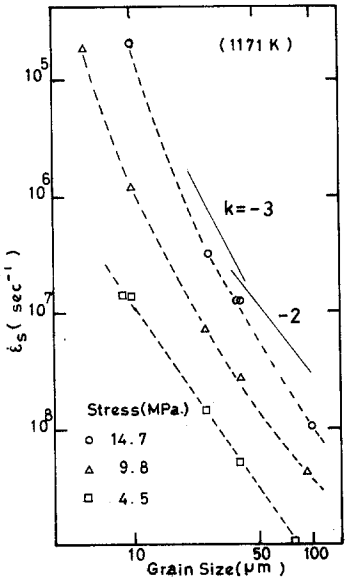

Figure 9 Grain-size dependence of $\dot{\varepsilon}_s$ at 1171 K for type 310 stainless steel.

the glide of dislocations within grains and the grain-boundary sliding, which occurs as an accommodation process. The flow within grains is interpreted in terms of a glide-recovery model [25, 26]. If this flow is controlled by the glide rate, the activation energy for creep can be modified by the thermal component of the applied stress and the thermal activation area, rather than by the temperature dependence of the elastic modulus [27]. Here is a reason why the activation energy for creep in the coarse-grained specimens is much larger in the stress range 9.8 to 19.6 MPa than that of the volume self-diffusion. In the case of $\sigma = 4.9$ MPa, $d = 600\,\mu$m, there is a possibility that the climb-recovery process is rate controlling, since the relationship of $\dot{\varepsilon}_s \propto \sigma^5$ is established and Q_c is similar to the activation energy of the volume self-diffusion of Fe, which cannot be explained only by either a vacancy creep model or a glide-recovery model.

The thermal and athermal components of the applied stress are necessary for an understanding of the creep behaviour within grains [27, 28]. The measurements of these components are in progress.

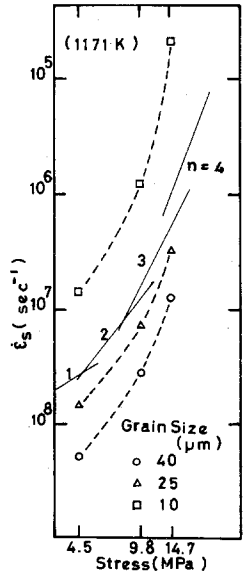

Figure 10 Stress dependence of $\dot{\varepsilon}_s$ at 1171 K for type 310 stainless steel.

References

1. C. L. CLARK and J. W. FREEMAN, *Trans. ASM* 38 (1947) 148.
2. G. J. GUARNIERI, J. MILLER and F. J. VAWTER, *ibid* 42 (1950) 981.
3. Y. IMAI and Y. FUJIMURA, *Jap. Inst. Metals* 29 (1) (1965).
4. Y. FUKASE, T. NISHIMA, K. EBATO and N. OKUBO, *J. Iron Steel Inst. Japan* 53 (1967) 820.
5. Y. FUKUI, R. SASAKI, F. HATAYA and S. TAKAHASHI, *ibid* 64 (1978) 478.
6. F. GAROFALO, W. F. DOMIS and F. VON GEMMINGEN, *Trans. Met. Soc. AIME* 230 (1964) 1460.
7. R. RAJ and M. F. ASHBY, *Met. Trans.* 2A (1971) 1113.
8. F. W. CROSSMAN and M. F. ASHBY, *Acta Met.* 23 (1975) 425.
9. R. C. GIFKINS, *Met. Trans.* 7A (1976) 1225.
10. P. SHAHINIAN and J. R. LANE, *Trans. ASM* 45 (1953) 177.
11. K. BORGGREEN and A. R. THÖLÉN, *Met. Trans.* 7A (1976) 1615.
12. J. E. DORN, *J. Mech. Phys. Solids* 3 (1954) 85.
13. C. M. YOUNG, S. L. ROBINSON and O. D. SHERBY, *Acta Met.* 23 (1975) 633.
14. C. R. BARETT, J. L. LYTTON and O. D. SHERBY, *Trans. Met. Soc. AIME* 239 (1967) 170.
15. K. R. WILLIAMS and I. R. McLAUCHLIN, *J. Mater. Sci.* 5 (1970) 1063.
16. B. RUSSELL, R. K. HAM, J. M. SILCOCK and G. WILLOUGHBY, *Met. Sci. J.* 2 (1968) 201.
17. T. ISHII, T. SHINODA and R. TANAKA, *J. Iron Steel Inst. Japan* 64 (1978) 469.
18. C. CRUSSARD and R. TAMHAKER, *Trans. Met. Soc. AIME* 212 (1958) 718.
19. A. F. SMITH and G. B. GIBBS, *Met. Sci. J.* 2 (1968) 47.
20. M. F. ASHBY, *Acta Met.* 20 (1972) 887.
21. G. CROSSLAND and R. B. JONES, *Met. Sci. J.* 11 (1977) 504.
22. E. EVANS, *Scripta Met.* 2 (1968) 157.
23. B. BURTON, *Phil. Mag.* 25 (1972) 645.

24. D. J. TOWLE and H. JONES, *Acta Met.* **24** (1976) 399.
25. W. D. NIX and C. R. BARRETT, *Trans. ASM* **61** (1968) 695.
26. A. A. SOLOMON and W. D. NIX, *Acta Met.* **18** (1970) 863.
27. O. K. CHOPRA and K. NATESAN, *Met. Trans.* **8A** (1977) 633.
28. S. TAKEUCHI and A. S. ARGON, *J. Mater. Sci.* **11** (1976) 1542.

Received 13 August and accepted 16 November 1978